Journal of Ceramic Processing Research. Vol. 9, No. 2, pp. 93~96 (2008)

J O U R N A L O F
Ceramic Processing Research

Curvature and bifurcation of MgO-Al_2O_3 bilayer ceramic structures

Chang Soo Kim and Stephen J. Lombardo*

Department of Chemical Engineering, University of Missouri, Columbia, MO 65211, USA

Ceramic bilayer structures are formed by coating a green alumina substrate with an aqueous magnesia slurry and then heating the composite body. At high temperature, diffusion and reaction to a spinel can occur, and the body deforms. The deformation of the bilayer structure is attributed to the phase change accompanying spinel formation and to differential sintering between layers. As compared to other bilayer structures obtained by deposition methods, relatively thick top layers are obtained and large strain mismatches occur. At small ratios of the thickness of the top to bottom layer for bilayer plates, equal curvature is observed in two directions whereas at larger thickness ratios, a bifurcation in the deformation behavior is observed with unequal curvature in two directions.

Key words: ceramic material, layered materials, bifurcation.

Introduction

In earlier work, we have developed a ceramic forming method based on strain-induced *in situ* deformation of green bodies, without the application of external pressure [1-4]. The forming method (see Fig. 1) is practiced by applying an oxide coating onto an alumina substrate and then heating the composite body to high temperature. As a consequence of the heating cycle, the coating can diffuse into and react with the substrate, at which point deformation can occur. This forming method has been demonstrated for chromia, magnesia, calcia, and silica coatings on dense and green alumina substrates. An example of a ceramic wave spring formed by this method is shown in Fig. 1.

During the development of this forming method, the substrate geometry was initially confined to a beam shape to simplify the analysis of the underlying mechanism. In these earlier studies, curvatures of up to 0.1 mm^{-1} were observed and linear deformation models suggested that large strain mismatches of up to 5-7% were driving the deformation [2,3]. Based on the occurrence of such curvatures and strains, we have investigated the bending behavior of bilayer ceramic plates for different ratios of thickness of the top to bottom layers. For the plate geometry, we have observed a bifurcation in the bending behavior, as has been observed in other bilayer systems [5-13]. Such bilayer systems often exhibit a region of equal curvature in two directions at low thickness ratios, and as the thickness ratio increases, a critical thickness ratio is achieved at which point unequal curvature in two directions is observed. Such behavior is also seen for the ceramic bilayer structures studied here.

*Corresponding author:
Tel : + 573 884-1644
Fax: + 573 884-4940
E-mail: Lombardos@missouri.edu

Experimental

A schematic of the forming process is shown in Fig. 1, and has been described in more detail elsewhere [2,3]. Alumina (Alcoa A-16, Bauxite, AR) tapes were fabricated by tape-casting from aqueous alumina slurries. After drying, the tapes were cut into beams of 40 mm length and 1.5 mm width at different thicknesses. Plates were fabricated with dimensions of 40 mm length, 10 mm width, and thicknesses ranging from 200 μm to 2000 μm. For the thicker substrates, slip casting was used as the forming method. The binder used in the forming process was removed by thermal heat treatment in air in a box furnace. After binder removal, an aqueous-

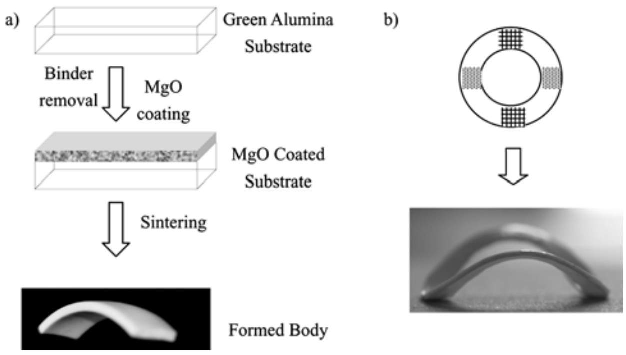

Fig. 1. a) Schematic of the processing method used to introduce curvature into a flat substrate. The sample in the image has dimensions of 34 × 8.5 × 0.6 mm. b) Example of a wave spring formed by applying a SiO_2 coating on a green alumina substrate in an alternating top and bottom fashion (see shaded regions) at 90° intervals. The dimensions of the wave spring are 25 mm in diameter, width of 5 mm, and thickness of 0.6 mm.

based slurry of magnesia (Aldrich, St. Louis, MO, ~325 mesh) was coated at a concentration of 1.5 mmol/mm^2 on the top surface of the alumina substrate. The magnesia coated alumina substrates were then heated in air in a box furnace with a ramp of 10 K minute^{-1} and a hold at 1600°C for 4 h, followed by controlled cooling to 200°C and then free cooling to room temperature. During exposure of the samples to elevated temperature, the samples decreased in dimensions by approximately 15%. The microstructures of the samples were characterized by scanning electron microscopy (SEM) and energy dispersive spectroscopy (EDS).

To determine the curvature, two procedures were used. As seen in Fig. 1a, the curvatures of the beam samples were fairly uniform in both directions in the sample. Values of small curvature for the beam samples were obtained by measurement of the total deflection, W, and the sample arc length, L, with the equation $\kappa = [1-\cos(L\kappa/2)]/W$. For large deformation, the curvature was determined by direct measurement of the radius of curvature. The curvature values for plates showed more variation in each direction as compared to the beam samples, and in some instances exhibited non-uniform curvature in a direction.

Results

Alumina beam specimens of 40 mm length, 1.5 mm width, and different thicknesses were coated with magnesia and heated to 1600°C for 4 h. For these beam specimens, curvatures of up to 0.1 mm^{-1} were obtained, depending on the thickness ratio of the coating to substrate. The microstructure of a beam sample processed in this manner is shown in the SEM image in Fig. 2, where a bilayer structure is evident. A more dense top layer of thickness h_1 = 70 µm is clearly distinguishable from the more porous balance of the substrate thickness, denoted as h_2.

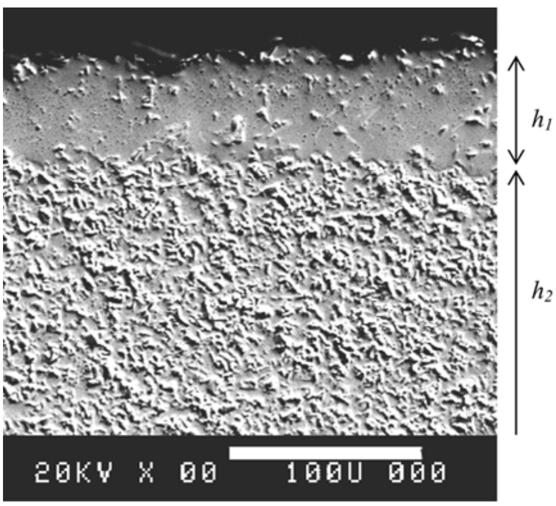

Fig. 2. SEM micrograph of an MgO coated alumina substrate held at 1600°C for 4 h. Two regions, denoted as h_1 and h_2, are evident.

Compositional profiling by EDS across the thickness of the substrate is shown in Fig. 3. A relatively constant MgO/Al_2O_3 molar ratio between 0.5-0.7 is seen followed by a sharp decrease to an alumina rich balance of the substrate beyond 70 µm. The thickness of the MgO-rich region from EDS is consistent with the location of the interface separating the h_1 and h_2 regions seen in the SEM micrograph in Fig. 2. The MgO/Al_2O_3 molar ratio of 0.5-0.7 corresponds to the spinel phase field [14], and the presence of spinel has been verified by scanning x-ray diffraction [2]. The relatively constant MgO/Al_2O_3 concentration can be explained by a process governed by reaction control, as compared to diffusion control [15,16]. The sharp delineation between MgO-rich and MgO-poor regions of the samples seen here has also been observed for $MgO\text{-}Al_2O_3$ diffusion couples [16,17]. The results in Figs. 2 and 3 thus suggest that the ceramic beams can be treated as bilayer structures.

Alumina substrates of plate geometry were coated with a constant amount of magnesia at 1.5 mmol/mm^2 in a similar fashion to the beam substrates and then were heated to 1600°C for 4 h. The curvature behavior of three plates of different thickness is shown in Fig. 4. For the plate with an h_1/h_2 thickness ratio of 0.04 seen in Fig. 4a, the curvatures in the long x-direction and shorter y-directions are similar. For the thinner plate in Fig. 4b, *e.g.,* a higher thickness ratio, the plate has buckled, and the dominant curvature is now in the shorter y-direction. As the thickness ratio further increases as in Fig. 4c, κ_x approaches zero and at the same time, κ_y increases and more buckling of the specimen is observed. In fact, for the 1.93 thickness ratio in Fig. 4c, the original plate has now deformed into a structure consisting of two parallel partial tubes which impinge on the substrate. For such structures, the reported

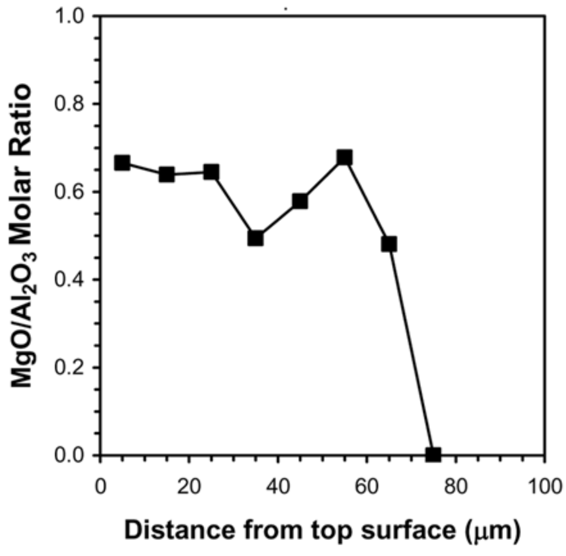

Fig. 3. MgO/Al_2O_3 molar ratio, as determined by EDS, with depth for green alumina substrates coated with MgO and held at 1600°C for 4 h.

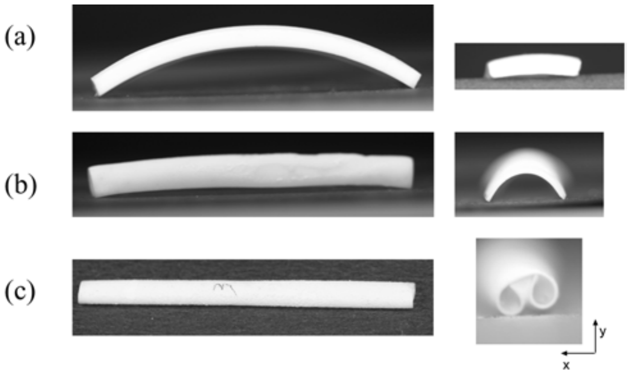

Fig. 4. Photos of the curvature of plate samples fabricated at different h_1/h_2 thickness ratios of (a) 0.04, (b) 0.28, and (c) 1.93. The photos on the left show the curvature along the x-direction (sample length is 34 mm), and the photos on the right show the curvature along the y-direction (sample width is 8.5 mm).

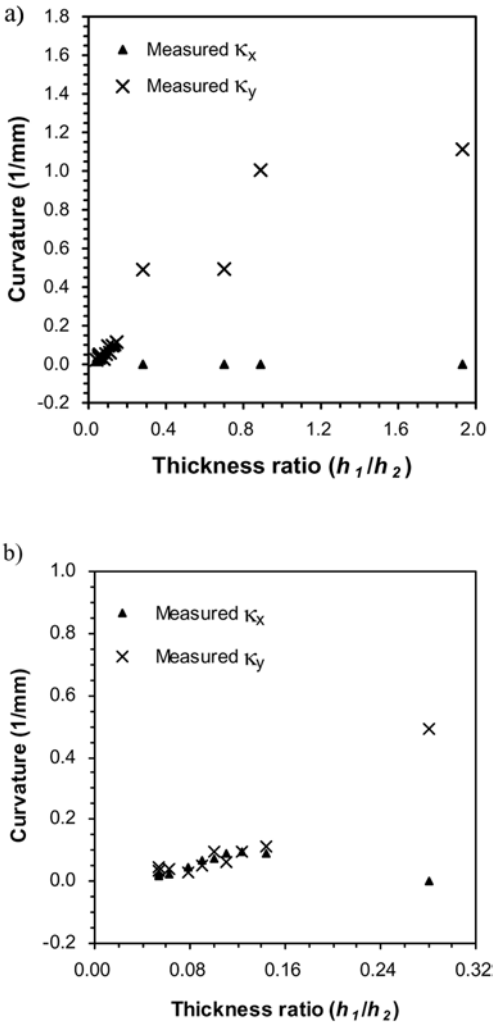

Fig. 5. a) Curvature in the x- and y-directions of plate specimens versus thickness ratio. b) Enlargement of the area for small thickness ratios from panel a).

curvature represents the larger values. The buckling behavior evident in Figs. 4b and 4c indicates that a mechanical bifurcation has occurred, which results in different curvature in different directions within the plates.

The measured curvatures in the two directions in biceramic plates fabricated as described above are presented in Fig. 5 as a function of the thickness ratio. Until a thickness ratio of 0.14, the curvatures in each direction are very similar and both increase with increasing thickness ratio. As the thickness ratio increases, a critical bifurcation point is reached where the two curvatures diverge, which is a trend seen in other bilayer structures as well [5-13]. Beyond a thickness ratio of 0.28, the two curvatures diverge drastically, where κ_x in the long direction is almost zero and κ_y in the shorter direction exceeds 0.5 mm^{-1}. Figure 5b demonstrates clearly that until a thickness ratio of $h_1/h_2 \approx 0.14$, the curvatures in both the x- and y-directions are equal.

Discussion

The ceramic bilayer system examined here differs in a number of ways from the often-studied bilayer structures obtained by depositing metals on glass or ceramic substrates [5-7]. For metal deposition, the magnitude of the observed curvature, κ, is often much less than 0.1 mm^{-1}, whereas for the ceramic forming method used here, curvatures of more than 0.1 mm^{-1} and up to 1 mm^{-1} are routinely achieved. For the deposition methods, the intrinsic strain driving the curvature is less than 1%, whereas linear deformation models suggest that strain mismatches of up to 5-7% are driving the deformation of the ceramic bilayer structures. Thicker substrates and thicker coatings can also be realized with the ceramic bilayer forming method, as compared to what is practiced for metal deposition on substrates. The limitations for the metal deposition process arise, in part, because of the propensity for delamination of the deposited layer from the substrate. For the ceramic bilayer forming method, the process of sintering may promote better mechanical integrity between the two layers, thereby allowing for more curvature to occur without delamination.

Another difference arises from consideration of the driving force for deformation. For metal coatings deposited on glass or ceramic substrates, the driving force for deformation is often expressed as a coefficient of thermal expansion (CTE) mismatch that arises upon cooling. For ceramic bilayers formed by coating magnesia on alumina, the driving force for deformation has been attributed to strain mismatch arising from the formation of a new phase, spinel, and from differential sintering between the layers. The former driving force is quite large, and is actually opposed by the effect of differential sintering. Although CTE effects for the ceramic bilayers are expected to be operative during cooling from high temperature, the magnitude of the CTE mismatch is insufficient to account for the large curvatures obtained, and in fact is an order of magnitude lower than the calculated strain mismatches of 5-7% [2, 3]. In addition, for the specific case of a spinel layer on alumina, the direction of bending observed in the experiments is opposite to what would be predicted based on CTE mismatch alone. Ultimately, however, from a mechanics viewpoint, the precise driving force is not important but rather it is the distribution of mismatch strain and material properties that determines the curvature.

A final difference between the deposition methods and the ceramic forming method described here is related to the underlying mechanics of deformation. For the deposition approaches, elastic mechanics are used to describe the deformation, which is cast as arising from a CTE mismatch during cooling. For the ceramic forming method, a body of literature has indicated that alumina behaves viscously at elevated temperature [18-21]. As the substrates examined here are predominantly alumina, their deformation behavior at high temperature is likely viscous as well.

In spite of these differences in driving forces and deformation mechanics, the bilayer structures formed here exhibit some similarities as compared to other bilayer systems. At small thickness ratios, equal curvature is observed in both directions, whereas at larger thickness ratios, a critical bifurcation thickness ratio is achieved beyond which the curvature becomes unequal in two directions. The similarity in deformation behavior observed for this viscous ceramic forming method, as compared to systems behaving elastically, may not be surprising, however, in light of the visco-elastic analogy [18-22], whereby the governing equations for elastic response can be reformulated to describe visco-elastic response.

Conclusions

Structures fabricated by coating magnesia on alumina substrates have been shown to undergo large deformation after exposure to high temperature. The underlying microstructure exhibits a bilayer structure, which arises from a reaction-controlled mechanism between the magnesia coating and the alumina substrate. Upon exceeding a critical thickness ratio of the two layers, bifurcation in the curvature behavior occurs. Beyond the critical bifurcation point, the largest curvature was always along the short direction of the rectangular plates for all of the thickness ratios examined here.

Acknowlegement

This work was supported by the National Science Foundation under Grant No. 0203136.

References

1. S. J. Lombardo, D. Bianchi, B. Bishop, A. Giannakopoulos, R. Goldsmith, R. Higgins, R. Pober, and S. Suresh, J. Am. Ceram. Soc. 82[6] (1999) 1401-1408.
2. C. S. Kim, R. A. Winholtz, and S. J. Lombardo, J. Am. Ceram. Soc. 88[8] (2005) 2064-2070.
3. C. S. Kim and S. J. Lombardo, J. Am. Ceram. Soc. 89[9] (2006) 2718-2725.
4. C. S. Kim and S. J. Lombardo, J. Ceram. Process. Res. 8[1] (2007) 43-51.
5. B. D. Harper and C. P. Wu, Int. J. Sol. Struct. 26[5/6] (1990) 511-525.
6. L. B. Freund, A. J. Rosakis, and H. S. Lee, in AMD-Vol. 236, Finite Thermoelasticity, Proceedings of the ASME International Mechanical Engineering Congress and Exposition (American Society of Mechanical Engineers, New York, 1999) 1-13.
7. L. B. Freund, J. Mech. Phys. Solids 48 (2000) 1159-1174.
8. C. B. Masters and N. J. Salamon, Int. J. Eng. Sci. 31[6] (1993) 915-925.
9. C. B. Masters and N. J. Salamon, J. Appl. Mech. 61 (1994) 872-878.
10. N. J. Salamon and C. B. Masters, Int. J. Sol. Struct. 32[3/4] (1995) 473-481.
11. M. W. Hyer, J. Comp. Mater. 15 (1981) 296-310.
12. M. Finot and S. Suresh, J. Mech. Phys. Solids 44[5] (1996) 683-721.
13. N. Guyot, Y. Harmand, and A. Mezin, Int. J. Sol. Struct. 41 (2004) 5143-5154.
14. B. Hallstedt, J. Am. Ceram. Soc. 75[6] (1992) 1497-1502.
15. W. P. Whiteny II and V. S. Stubican, J. Am. Ceram. Soc. 54[7] (1971) 349-352.
16. P. Zhang, T. DebRoy, and S. Seetharaman, Metal. Trans. 27A (1996) 2105-2114.
17. R. E. Carter, J. Am. Ceram. Soc. 44[3] (1961) 116-120.
18. R. K. Bordia and G. W. Scherer, Acta Metal. 36[9] (1998) 2393-2397.
19. R. K. Bordia and G. W. Scherer, Acta Metal. 36[9] (1988) 2399-2409.
20. P. Z. Cai, D. L. Green, and G. L. Messing, J. Am. Ceram. Soc. 80[8] (1997) 1929-1939.
21. P. Z. Cai, D. L. Green, and G. L. Messing, J. Am. Ceram. Soc. 80[8] (1997) 1940-1948.
22. W. N. Findley, J. S. Lai, and K. Onaran, Creep and Relaxation of Nonlinear Viscoelastic Materials (North-Holland Publishing Company, New York, 1976).